



# Automated Detection of Alzheimer's Disease Using Brain MRI Images– A Study with Various Feature Extraction Techniques

U. Rajendra Acharya<sup>1,2,3</sup> · Steven Lawrence Fernandes<sup>4</sup> · Joel En Wei Koh<sup>1</sup> · Edward J. Ciaccio<sup>5</sup> · Mohd Kamil Mohd Fabell<sup>6</sup> · U. John Tanik<sup>7</sup> · V. Rajinikanth<sup>8</sup>  · Chai Hong Yeong<sup>2</sup>

Received: 20 January 2019 / Accepted: 21 July 2019 / Published online: 9 August 2019  
© Springer Science+Business Media, LLC, part of Springer Nature 2019

## Abstract

The aim of this work is to develop a Computer-Aided-Brain-Diagnosis (CABD) system that can determine if a brain scan shows signs of Alzheimer's disease. The method utilizes Magnetic Resonance Imaging (MRI) for classification with several feature extraction techniques. MRI is a non-invasive procedure, widely adopted in hospitals to examine cognitive abnormalities. Images are acquired using the T2 imaging sequence. The paradigm consists of a series of quantitative techniques: filtering, feature extraction, Student's t-test based feature selection, and k-Nearest Neighbor (KNN) based classification. Additionally, a comparative analysis is done by implementing other feature extraction procedures that are described in the literature. Our findings suggest that the Shearlet Transform (ST) feature extraction technique offers improved results for Alzheimer's diagnosis as compared to alternative methods. The proposed CABD tool with the ST + KNN technique provided *accuracy of 94.54%, precision of 88.33%, sensitivity of 96.30% and specificity of 93.64%*. Furthermore, this tool also offered an accuracy, precision, sensitivity and specificity of 98.48%, 100%, 96.97% and 100%, respectively, with the benchmark MRI database.

**Keywords** Brain MRI · Alzheimer's disease · Feature extraction · KNN classifier · Performance evaluation

## Introduction

Alzheimer's disease (AD), the most widespread reason for dementia in the elderly, is a chronic degenerative disease with progressive loss of intellectual function. The cognitive decline is characterized by gradual disappearance of healthy nerve cells in the cerebral cortex, especially in the frontal and medial temporal regions of the brain. AD is also a significant factor in morbidity, ranked fifth among causes of death by the World

Health Organization (WHO) [1]. The presence of amyloid plaques and neurofibrillary tangles in the brain are characteristic features of this disease. Although the cause of AD is poorly understood, the risk factors include genetics, history of head injury, depression, and hypertension. AD is also found to occur in people with Down's syndrome about 20 years earlier than the general population [2]. The onset of the disease is subtle and usually occurs when over 65 years of age. The first noticeable changes include difficulty in short term

---

This article is part of the Topical Collection on *Image & Signal Processing*

---

✉ V. Rajinikanth  
v.rajinikanth@ieee.org

<sup>1</sup> Department of Electronics and Computer Engineering, Ngee Ann Polytechnic, Singapore, Singapore

<sup>2</sup> School of Medicine, Faculty of Health and Medical Sciences, Taylor's University, 47500 Subang Jaya, Malaysia

<sup>3</sup> Department of Biomedical Engineering, School of Science and Technology, Singapore University of Social Sciences, Singapore, Singapore

<sup>4</sup> Department of Electronics and Communication Engineering, Sahyadri College of Engineering & Management, Mangaluru, India

<sup>5</sup> Department of Medicine, Columbia University, New York, NY, USA

<sup>6</sup> Department of Biomedical Imaging, Faculty of Medicine, University of Malaya, Kuala Lumpur, Malaysia

<sup>7</sup> Department of Computer Science and Information Systems, Texas A&M University-Commerce, Commerce, TX, USA

<sup>8</sup> Department of Electronics and Instrumentation, St. Joseph's College of Engineering, Chennai 600119, India

memory, disorientation, lack of self-care, behavioral changes, depression, anxiety, and problems with language. It is generally accepted that Alzheimer's disease has a gradual and irreversible progression. In the terminal stages of the disease, the patient may lose ability to perceive, think, speak or move, ultimately leading to loss of bodily functions and then finally to death. The progression of the disease may take from 3 to 9 years [3, 4], or even longer.

The stages of AD include pre-dementia, early stage, middle stage, and advanced stage. The symptoms of the pre-dementia stage mimic the process of normal aging, including forgetfulness with mild cognitive impairment. In the early stages, impairment of learning, executive function, and memory are more prominent, often resulting in some language difficulty. In the middle stage, speech difficulties become more evident, reading and writing skills are progressively attenuated, and long-term memory also becomes impaired. In the advanced stage, Alzheimer's patients may exhibit apathy and simpler tasks cannot be carried out independently; the afflicted individual eventually becomes bedridden, and ultimately death ensues [5, 6].

The diagnosis of AD is based on the history of the illness and the presence of neurological and psychological features. The medical history of the patient may be obtained from relatives, and the behavior of the patient can also be assessed [7]. The dietary pattern, as well as use of medicines and other supplements by the patient, is also taken into consideration during the screening for Alzheimer's disease. Advanced medical imaging includes Computed Tomography (CT), Magnetic Resonance Imaging (MRI) and Positron Emission Tomography-Computed Tomography (PET-CT) techniques. A CT scan helps to diagnose dementia by checking the size of various regions of the brain, counting the temporal lobe, hippocampus, and frontal lobe. The MRI scan of the brain shows the brain structures, shrinkage of the brain, vascular irregularities, and any other structural changes that might cause cognitive dysfunction. Memory loss caused by stroke or tumors can be ruled out by MRI scans. PET-CT of various types of brain functions are widely available: (i) fluorodeoxyglucose (FDG) PET-CT are used to measure the brain glucose levels, (ii) amyloid PET-CT are used to measure beta-amyloid proteins, and (iii) tau PET-CT are used to detect tau, the protein that forms neurofibrillary tangles in nerve cells [8, 9]. For instance, a positive amyloid PET-CT scan (higher levels of beta-amyloid) would be helpful to confirm AD. These diagnostic methods can also be useful to rule out other conditions that might contribute to dementia, such as tumors, stroke, and head trauma [10].

The primary role of MRI in the analysis of AD is the evaluation of volume alteration in characteristic positions, which can offer an analytical accuracy of up to 87% [11, 12]. The appraisal is frequently done on mesial temporal lobe atrophy (i.e. hippocampus and entorhinal cortex) and temporoparietal

cortical atrophy. Mesial temporal lobe atrophy can be estimated directly or indirectly. Direct estimation is based on measurement of the volume loss of hippocampal or parahippocampal tissue, while indirect estimation relies on the magnification of the parahippocampal fissures. These estimations are generally analyzed together with the medial temporal atrophy score, which has been shown to be predictive of progression from mild cognitive impairment to dementia. Early onset of AD can be detected through the presence of parietal atrophy on the interhemispheric surface by examining the subsequent cingulate sulcal and parietooccipitalsulcal dimension, and the degree of atrophy of the precuneus and cortical region in the parietal lobe.

The microscopic examination of brain tissue gives a definitive diagnosis of the disease. The cognitive impairments found in this disease are evaluated with neuro-psychological tests such as the Mini-Mental State Examination (MMSE) and Mini-Cog test [11]. Mood assessment of the patient to detect behavioral changes, such as anxiety or depression, is also carried out to rule out other ailments that overlap dementia [11, 12]. Although the confirmative diagnosis of AD can only be done in an autopsy by direct examination of the brain tissue, other indirect, yet effective methods are emerging. These include analyzing specific biomarkers that accurately assess the levels of amyloid proteins in cerebro-spinal fluid (CSF) and blood, which are being widely used to determine the current size of the brain and its functional state.

The clinical significance of AD, combined with the widespread availability of recent non-invasive imaging techniques, has attracted the attention of the research community in the field to advance reliable and accurate technical assessments for a myriad of brain conditions. In fact, a variety of Computer-Aided-Brain-Diagnosis (CABD) systems have been recently proposed and implemented by researchers to examine the occurrence and severity of AD [13–20]. The general framework of the CABD implemented for the AD includes (i) collection of brain imagery using a recommended imaging technique, (ii) implementation of image pre-processing techniques to enhance brain images, (iii) mining of vital features using a chosen feature extraction technique, (iv) assessing dominant feature selection, (v) implementing a classifier system to categorize the brain-image, and (vi) validation of the developed CABD using the brain MRI database.

In our study, a CABD system was developed and implemented to classify the selected T2-weighted brain MRI images into normal and AD cases. Initially, the pre-processing was implemented for the test images using a median filter, which helps to enhance the test pictures by removing noise. Thereafter, a feature extraction technique was implemented to mine the vital features from the brain MRI. In this work, a detailed relative study between the feature selection procedures, including the Contourlet Transform (CoT), Curvelet Transform (CuT), Complex Wavelet Transform (CWT),

Dual Tree Complex Wavelet Transform (DTCWT), Discrete Wavelet Transform (DWT), Empirical Wavelet Transform (EWT), and Shearlet Transform (ST), was implemented. Then Student's *t*-test was applied to select a subset of features based on the *p* value for classification. Finally, the *k*-Nearest Neighbor (KNN) classifier was implemented to classify brain MRI. The developed CABD system was tested using a  $256 \times 256$  pixel sized clinical dataset (110 normal cases and 55 AD cases) and benchmark images (30 normal and 30 AD cases). During the assessment, a 3-fold stratified Cross Validation (CV) procedure was implemented to validate the performance of the CABD system. The performance of the considered feature extraction procedures was determined by calculating the accuracy, precision, sensitivity, specificity, and F1 score.

The remaining part of this research work is structured as follows: section 2 outlines related research findings available in the literature; the relevant methods implemented to examine brain MRI are discussed in section 3. Section 4 presents the experimental results and discussion, and the conclusion of the present research work is discussed in section 5.

## Related work

In the domain of medical imaging, AD diagnosis is essential not only for preserving individual cognitive capacity, but also for public health in general. AD creates serious problems for human thinking, memory, and related living activities. Due to the unrelenting destruction of nerve cells over time, basic human intellectual abilities are severely impaired in the later stages of life [21]. In the USA alone, approximately five million people are affected by AD, mostly in the age group of 80–90 years [22]. For early detection of AD, various therapies and diagnostic techniques are being developed. Although MRI is a powerful tool that can be useful to recognize signs of AD in the brain, the acquisition procedure is time-consuming, primarily due to the need for manual inspection of workflow bottlenecks [23].

Recently, several techniques have been introduced for the diagnosis of AD using image processing and machine learning techniques, which perform more efficiently as compared with manual systems. Madhumitha et al. [24] presented a method for early diagnosis of AD using an MRI scan through an effective image processing technique. The atrophy is computed through K-means, wavelet, watershed, and a few other customized algorithms. The results of this approach may provide a helpful diagnostic measure for early stage AD. The work of Kaur and Kaur was to study several enhancement techniques which are utilized for AD detection [25]. The corrected red and green ingredients are used for this purpose, and the sensitivity and specificity were computed to determine the best approach for AD detection. Yue et al. [26] presented a new technique for AD detection using MRI through gradient

echo plural contrast imaging (GEPCI). This technique identifies those brain tissues which are damaged through AD. The GEPCI technique enhances the resolution of diseased areas in the MRI, which is helpful for measurement of brain tissues.

Sankari and Adeli [27] introduced a method for AD diagnosis by applying a probabilistic neural network (PNN) technique to MRI images. The atrophy rate and total brain volume are computed in the first stage. Then features are extracted, such as contrast, correlation, and shape, which are input to the classifier. In comparison, PNN outperforms SVM and KNN in terms of the accuracy, sensitivity, and specificity. Plant et al. [28] designed a novel framework for the prediction of AD using MRI images. They combined the three classifiers SVM, Bayes statistics, and voting feature interval (VFI) for matching the patterns of AD in the imagery. For this purpose, MRI was obtained from thirty-two AD patients, and features were duly extracted and discussed by Plant et al. [28]. Thereafter, feature selection was employed, and a significant prediction accuracy was shown. Zhang et al. [29] described a new machine learning based approach for AD detection using MRI images. Initially, skull stripping was performed for removal of extracted regions, and then stationary wavelet entropy based features were extracted. The extracted entropy features were input to a single hidden layer neural network (NN). Thereafter, weights and biases of NN were optimized via particle swarm optimization (PSO), which significantly improved the detection performance.

Wang et al. [30] described detection of AD using MRI through a single slice method along with wavelet entropy and perceptron learning (PL). In the feature extraction step, various features were obtained, including single slice features via ICV, wavelet transform, wavelet orientation, and wavelet entropy. The extracted features were then classified by a multilayer perceptron (MLP) with optimized performance through a biogeography-based algorithm. The detection results outperform as compared with the latest methods. Dong et al. [31] applied an undersampling method for AD detection from MRI images. They utilized principal component analysis (PCA) and singular value decomposition for feature extraction and prominent features selection. Finally, the support vector machine (SVM) and decision tree (DT) algorithms were fused to achieve significant performance. Zhang et al. [32] introduced an AD detection system using MRI images. The displacement field (DF) evaluation was computed to detect AD abnormalities in an otherwise normal brain. The DWT features were extracted and reduced by PCA. Later, reduced features were categorized by three classification methods including SVM, generalized eigenvalue proximal SVM, and twin SVM (TSVM), which demonstrated better performance. They concluded that DF is helpful in AD detection when utilizing MRI images.

Syed et al. [33] presented a hybrid approach for AD classification with MRI. Three primary steps were performed:

feature extraction, reduction, and classification. DWT features were extracted from MRI images and reduced by irrelevant points through PCA. Finally, they utilized ANN and KNN for classification into healthy and AD images. Wang et al. [34] described a new method for AD detection and classification through the Zernike moment (ZM) features and a linear regression (LR) classifier. Through ZM, features were extracted of length 10–256 for each MRI image. The extracted ZM features were finally classified by LR, reaching an accuracy of 97.51%, which is superior to existing methods [35]. Furthermore, Wang et al. [36] established that existing techniques do not achieve better accuracy for AD detection, and

do not properly classify AD-related areas. For this purpose, they presented a computerized method based on 3D DF estimation among healthy and AD groups. The features were extracted through the 3D DF method, while significant features were selected by using the Bhattacharyya distance (BD), Student's t-test, and Welch's t-test (WTT). The selected features were then classified by SVM and TSVM, yielding a notable performance. Zhang et al. [37] introduced a CAD system for the detection of AD from MR images. They selected key slices from 3D MRI images through maximum inter-class variance. Then eigenbrains were generated for each set of slices. Later, essential eigenbrains were computed through

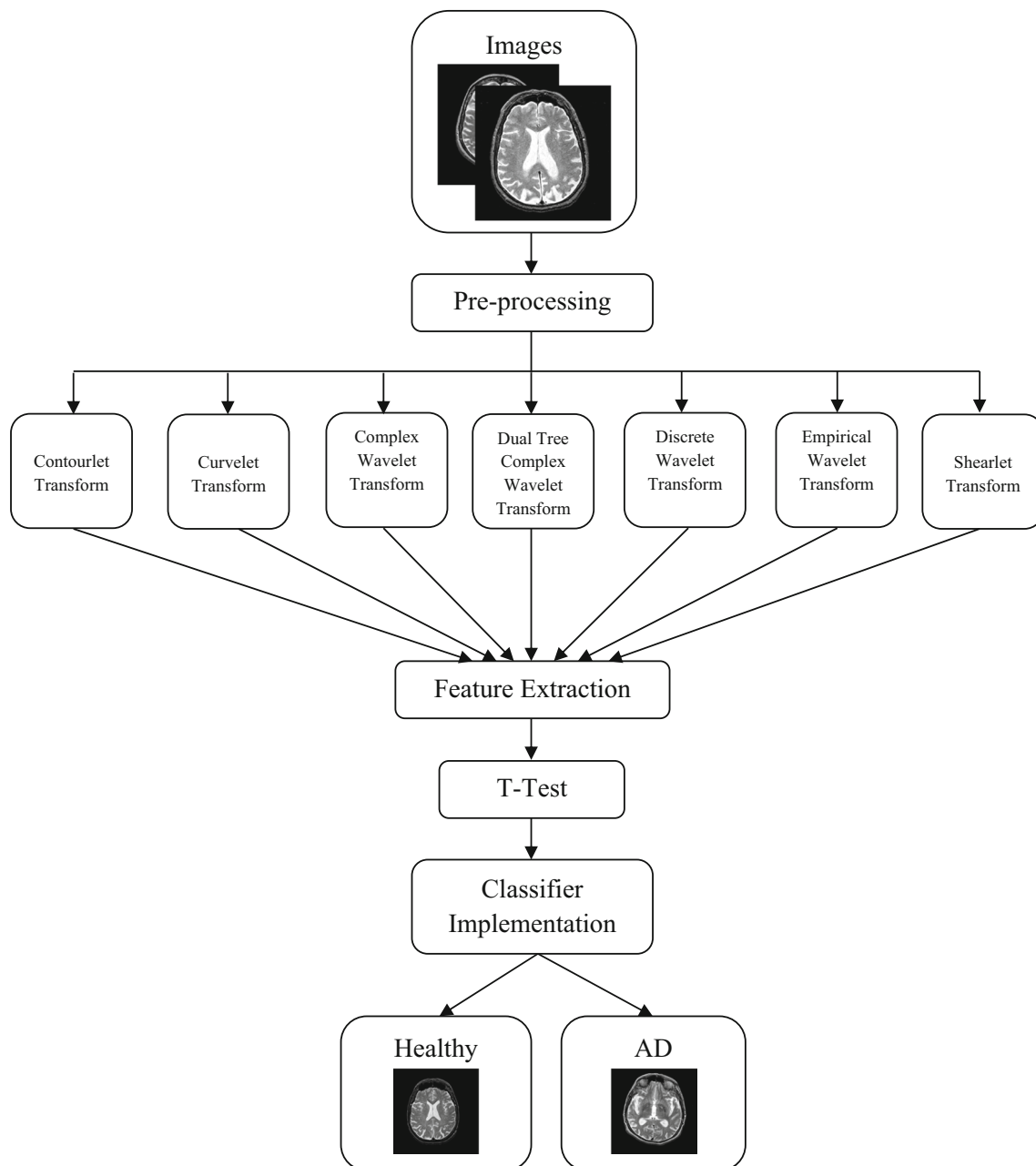


**Fig. 1** Structure of the CABD system proposed in this work

Welch's t-test, and input to SVM was done along various kernels. The prediction performance was improved further via the PSO algorithm. The introduced system outperformed, efficiently predicted AD, and discriminated brain regions.

Zhang et al. [38] described a CAD system for AD detection using MRI-scanned images. They extracted wavelet entropy and Hu moment invariant features from MRI images, and classification was performed via extraction of generalized eigenvalues proximal to SVM. The radial basis function (RBF) of SVM was used to increase the classification accuracy. Kette et al. [39] introduced a multi-textural (MTL) framework for feature extraction. Through the MTL approach, the structural information of AD was computed from an MRI image. Thereafter, they introduced an adaptive fusion method of various texture grading features extracted from the 3D Gabor filter. The classification results showed significant performance as compared with extant bio-marker techniques. Gao et al. [40] presented a deep learning-based method for AD classification. Through deep learning, significant information of AD was obtained at an early stage, which can be helpful for diagnosis. For deep learning architecture, both 2D and 3D Convolutional Neural Networks (CNN) are fused, yielding excellent performance based on Softmax scores.

The recent work of Ayadi et al. (2019) implemented a hybrid technique to extract features from selected brain MRI, and implemented a classifier system. This work considered the benchmark dataset of normal and disease classes including Alzheimer's disease (AD). Initially, the DWT technique was adopted to extract the features from the  $256 \times 256$  pixel sized test picture, and later the Bag-of-Words (BoW) concept was implemented to group the vital image features. Finally, a relative assessment among a range of classifiers, such as k-NN, RF, AB, and SVM, was implemented [58].

## Methodology

The methodology implemented in this study is depicted in Fig. 1. The main aim of the research was to develop a CABD system to classify normal versus AD cases, based on T2-weighted MRI brain images. Initially, the 2D test images of the brain MRI were collected from the University of Malaya Medical Centre (Medical Ethics Approval No. 2017112–5771) and the Harvard Brain Atlas [41]. During this process, 66 two-dimensional (2D) test images with dimension  $256 \times 256$  pixels were collected for the examination as discussed in Ayadi et al. (2019). Thereafter, a pre-processing procedure was implemented to enhance the test pictures considered for the study. The pre-processing implements a median filtering algorithm to remove noise and defects from the test picture [42, 43]. Thereafter, features were collected from the brain images using mining procedures described in the literature. The dominant features were then identified using the  $p$  value obtained with Student's t-test [44, 45]. Finally, the KNN classifier process was implemented to classify the test picture based on its features. Lastly, the performance of the proposed CABD system was validated based on the percentage values of accuracy, precision, sensitivity, specificity, and F1 score.

## Data pre-processing

Brain MRI pre-processing often involves skull-stripping, and enhancement based on image thresholding and filtering [46, 47]. In this work, the median filter was implemented to enhance the test picture under study. The details related to the medial filtering can be found in [42, 43].

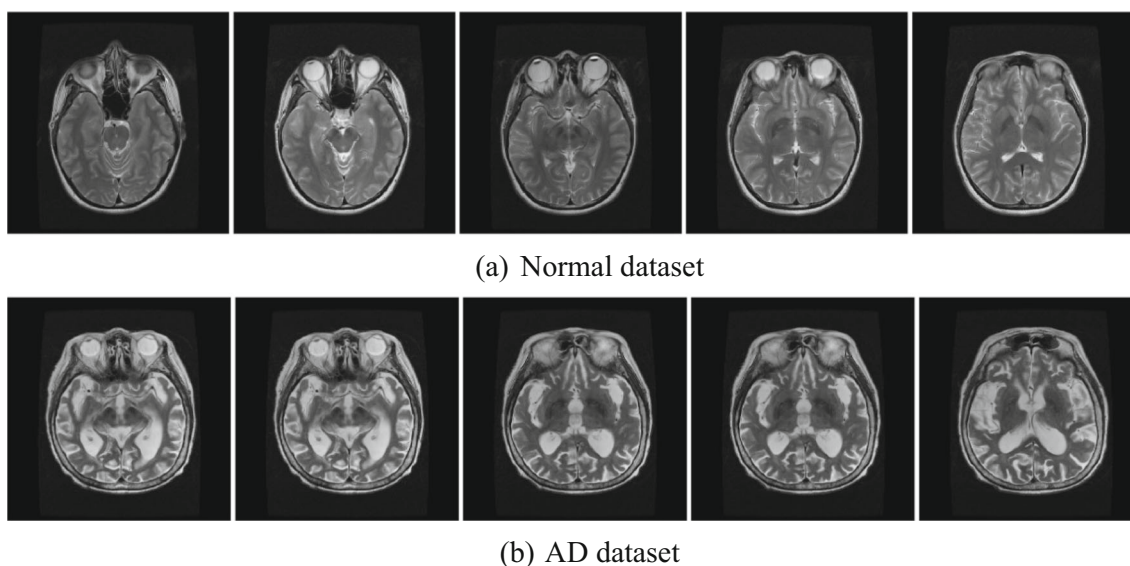


**Fig. 2** Sample test images considered from the clinical database

**Table 1** Clinical brain MRI dataset considered in this study

Image class	Number of MRI slices
Normal	22(subjects) × 5 (images/subject) = 110
AD	11(Patients) × 5(images/patient) = 55
Total	165

**Feature extraction**

The image features from the pre-processed brain MRI were initially mined using the Contourlet Transform (CoT). Later, a similar procedure was followed with other feature mining procedures including CuT, CWT, DTCWT, DWT, EWT and ST. These feature extraction techniques are widely adopted in a variety of signal and image processing scenarios [48–52]. A major objective of this research work was to develop a comparative analysis among the considered feature mining procedures, in order to identify the ideal feature mining technique that offers superior results. More details related to the adopted feature extraction techniques and their related application can be found elsewhere [53–57].

**Feature selection**

In the proposed CABD system, the feature selection process plays a vital role. In the literature, a variety of traditional and heuristic algorithm-based feature selection procedures are adopted to identify the leading features from the extracted features of each category. In this study, Student’s t-test was applied to select a subset of features based on the *p* value for classification, details of which can be accessed from previously published papers [44, 45].

**Table 2** Feature table using the Shearlet transform

Features	Normal		Alzheimer		Statistical measures	
	Mean	SD	Mean	SD	p Value	t-Value
S1O1_Vertical_Fuzzy Entropy	0.3238	0.1658	0.6944	0.1756	0.0000	5.8238
S2O5_Vertical_Yager Entropy	0.7553	0.1597	0.3315	0.2138	0.0000	5.8119
S1O9_Horizontal_Vadja Entropy	0.5265	0.1874	0.2137	0.1344	0.0000	5.4949
S2O4_Vertical_Yager Entropy	0.8146	0.1096	0.3824	0.2503	0.0001	5.4692
S1O1_Vertical_Max Entropy	0.6160	0.1724	0.2981	0.1513	0.0000	5.4267
S1O9_Vertical_Max Entropy	0.5410	0.1802	0.2274	0.1450	0.0000	5.3897
S1O9_Horizontal_Energy	0.5318	0.1927	0.2233	0.1369	0.0000	5.2973
S1O8_Vertical_Fuzzy Entropy	0.3265	0.1833	0.6921	0.1907	0.0000	5.2592
S1O7_Vertical_Fuzzy Entropy	0.3186	0.1536	0.6548	0.1830	0.0001	5.2378
S1O9_Horizontal_Fuzzy Entropy	0.3378	0.1871	0.6903	0.1809	0.0000	5.2163
S2O5_Vertical_Kapoor Entropy	0.2836	0.1669	0.7055	0.2412	0.0001	5.2111
S1O2_Vertical_Fuzzy Entropy	0.3011	0.1701	0.6475	0.1855	0.0001	5.1956
S1O9_Horizontal_Max Entropy	0.5326	0.1934	0.2143	0.1512	0.0000	5.1799
S1O9_Horizontal_Kapoor Entropy	0.5731	0.2111	0.2501	0.1454	0.0000	5.1393

**Classification**

From the literature, it is noted that the examination ability of the CABD system mainly depends on the type and quality of classifier system. Quite a few classifier systems exist in the field of brain MRI examination, but in this work only the well-known KNN technique was implemented to classify the brain MRI into normal versus AD [58]. Like other classifiers, KNN also needs training and testing based on image features.

KNN extrapolates the distance from a range of new data to all training data points, and finds the shortest distance as the best neighbour. The k value is empirically determined using the training sample’s sorting error.

The mathematical expression of the KNN implemented in this work is as follows:

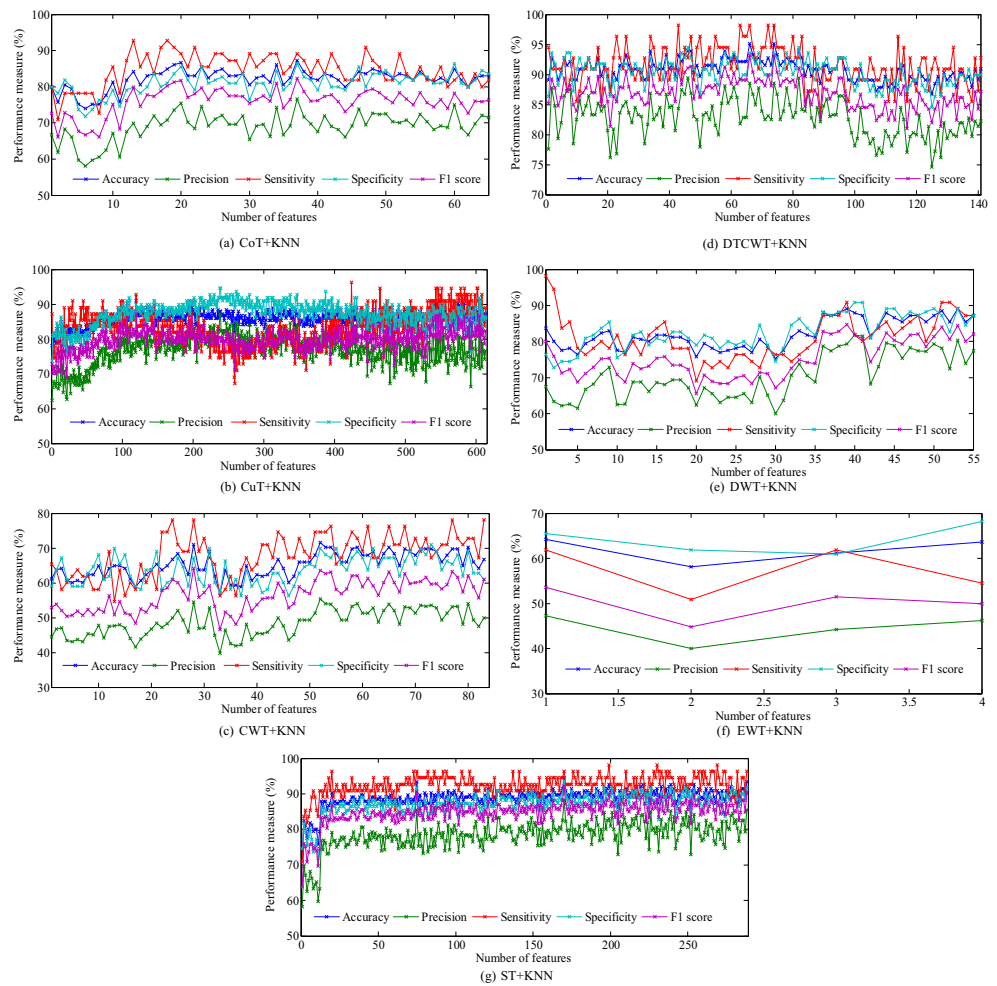
Let there exist two feature vectors of D dimensions,  $M = (M_1, M_2, \dots, M_n)^T$  and  $N = (N_1, N_2, \dots, N_n)^T$ , then the Euclidean distance can be shown to be:

$$\text{Euclidean distance}(\vec{M}, \vec{N}) = \sqrt{(M_1 - N_1)^2 + (M_2 - N_2)^2 + \dots + (M_D - N_D)^2} \tag{1}$$

**Validation**

The performance of the proposed CABD system was validated by computing well known image performance measures [46, 47]. In order to improve the examination capability, a three-fold cross validation was implemented. The performance values adopted in this work are depicted in Eq.’s (2) through (6).

**Fig. 3** Performance evaluation of the chosen feature extraction methods



$$Accuracy = (T_P + T_N) / (T_P + T_N + F_P + F_N) \tag{2}$$

$$Precision = T_P / (T_P + F_P) \tag{3}$$

$$Sensitivity = Recall = T_P / (T_P + F_N) \tag{4}$$

$$Specificity = T_N / (T_N + F_P) \tag{5}$$

$$F1\ Score = 2T_P / (2T_P + F_P + F_N) \tag{6}$$

where  $T_N$ ,  $T_P$ ,  $F_N$  and  $F_P$  signify true negative, true positive, false negative and false positive.

### Results and discussion

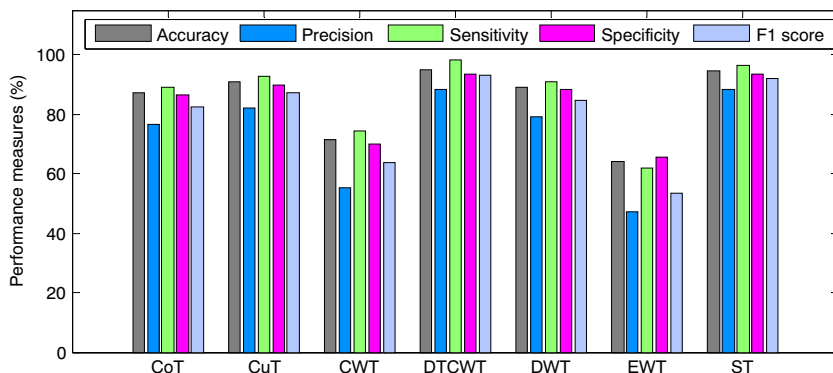
This section presents the experimental results and discussion. In this work, initially, the proposed approach is demonstrated on the clinical database. Figure 2 depicts normal and the AD-affected brain images collected from University of Malaya Medical Centre.

During image collection, every subject was separately examined. The images were selected from the axial T2-weighted

**Table 3** Performance evaluation of the feature extraction techniques

Feature extraction technique (No of Features)	TP	TN	FP	FN	Accuracy (%)	Precision (%)	Sensitivity (%)	Specificity (%)	F1 score (%)
CoT+KNN (38)	49	95	15	6	87.27	76.56	89.09	86.36	82.35
<b>CuT+KNN (121)</b>	51	99	11	4	<b>90.91</b>	<b>82.26</b>	<b>92.73</b>	<b>90.00</b>	<b>87.18</b>
CWT + KNN (53)	41	77	33	14	71.515	55.41	74.54	70.00	63.57
<b>DTCWT+KNN (67)</b>	54	103	7	1	<b>95.15</b>	<b>88.52</b>	<b>98.18</b>	<b>93.64</b>	<b>93.10</b>
DWT + KNN (40)	50	97	13	5	89.09	79.3	90.91	88.18	84.75
EWT + KNN (2)	34	72	38	21	64.24	47.22	61.82	65.45	53.54
<b>ST+KNN (171)</b>	53	103	7	2	<b>94.54</b>	<b>88.33</b>	<b>96.3</b>	<b>93.64</b>	<b>92.17</b>

**Fig. 4** Performance assessment of the clinical database



MRI sequence. The images were subjected to transformation and feature extraction, which was then formed into a single feature vector. Table 1 presents the details of the clinical dataset considered in this work.

After selecting the test images, a median filter was implemented to pre-process each image. Later, feature-extraction was implemented with the Shearlet Transform (ST). Feature selection was determined based on Student’s t-test. Finally, the KNN classifier was implemented and the results were verified. In this work, the training data were undersampled and used to train 1000 models, wherein the test set was verified with respect to the model in order to obtain a score assessing the degree of posterior probability. These probabilities were averaged together and used for class prediction. Like the ST, other feature extraction techniques were then implemented and tested separately on the clinical dataset.

Table 2 depicts the features extracted with the ST approach. Later, Student’s t-test based feature selection was implemented, and it was found that four features alone were sufficient to attain the expected result. This Table shows the *p* value and *t*-value obtained via comparison of mean between Normal and Alzheimer’s along with the statistical measures. Moreover, a 3-fold stratified Cross Validation (CV) was also implemented to attain better results during the brain MRI examination.

In this work, the feature mining and classification of the considered clinical images were incorporated using the considered feature extraction techniques and KNN based classification, and the corresponding results are depicted in Fig. 3. For this database, the CoT based feature extraction and classification was implemented with from 2 to 66 selected dominant features. The performance measure with reference to the number of chosen features is shown in Fig. 3a. Better

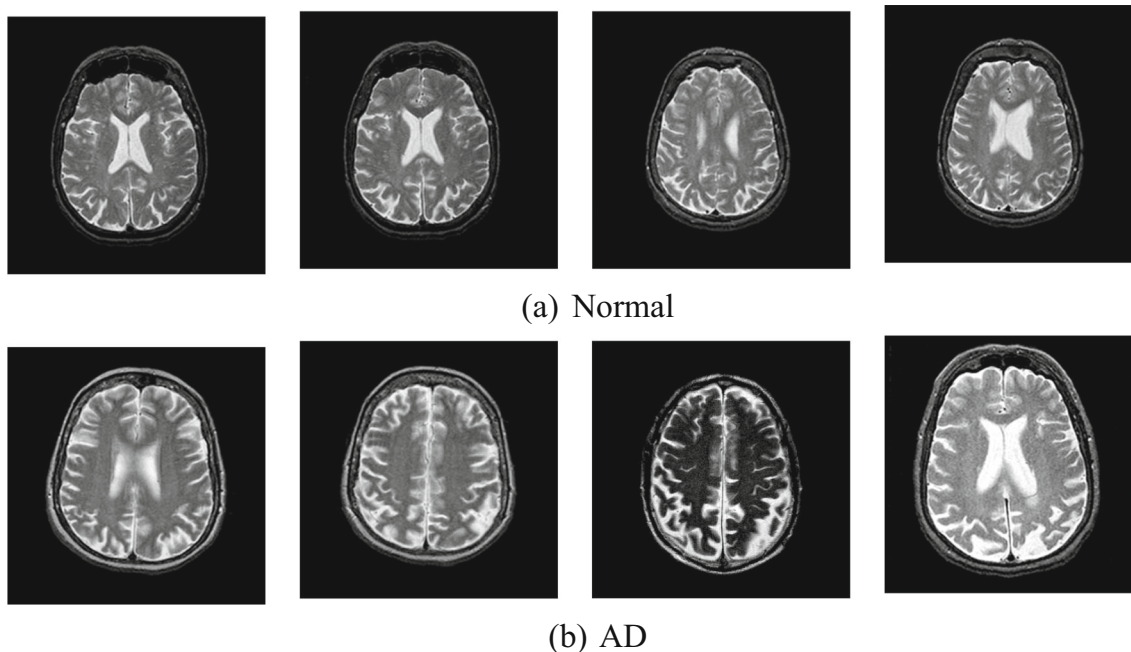


**Fig. 5** Test images of the Harvard Brain Atlas database



**Table 4** Performance evaluation with the benchmark database

Feature extraction technique (No. of Features)	TP	TN	FP	FN	Accuracy (%)	Precision (%)	Sensitivity (%)	Specificity (%)	F1 score (%)
CuT+KNN (6)	35	29	1	1	96.97	97.22	97.22	96.67	97.22
DTCWT+KNN (5)	34	29	1	2	95.45	97.14	94.44	96.67	95.77
<b>ST+KNN (5)</b>	<b>32</b>	<b>33</b>	<b>0</b>	<b>1</b>	<b>98.48</b>	<b>100.00</b>	<b>96.97</b>	<b>100.00</b>	<b>98.46</b>

performance measures were obtained when the number of features was selected as thirty-eight (dominant feature level), since the extracted features exhibit better classification

accuracy for both the normal and AD brain image cases. The performance values obtained with the CuT for 2 to 614 selected features are shown in Fig. 3b, and better performance

**Fig. 6** Dominant feature selection. **a** CuT, **b** DTCWT, **c** ST

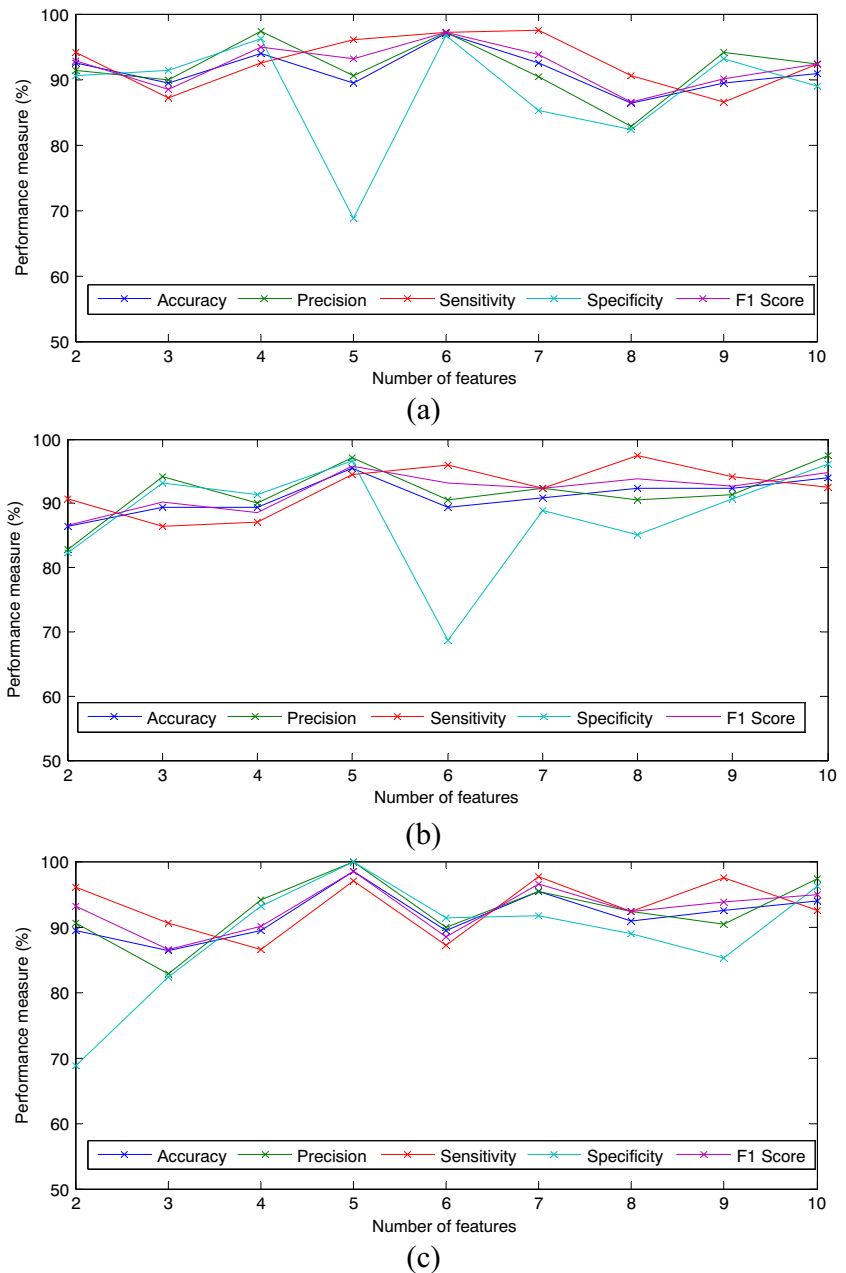
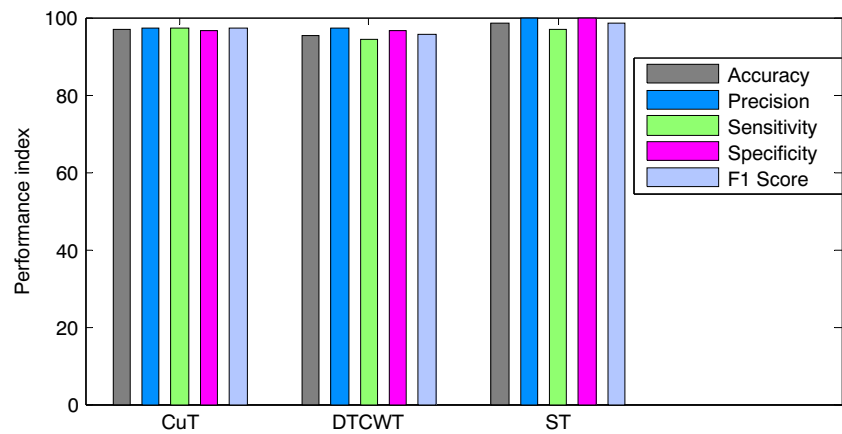


**Fig. 7** Performance evaluation for the benchmark database



values were obtained when the feature size is 121. Figure 3c depicts the performance measures obtained with the CWT approach for 2 to 84 features. In Fig. 3d, the performance obtained for the DTCWT procedure for 2 to 142 features is presented, and the better measures were attained when the selected feature size was 67. The outcome obtained with DWT for 2 to 56 features is shown in Fig. 3e. Figure 3f and g depicts the results obtained for 2 to 5 and 2 to 289 features, respectively.

Figure 3 depicts the various performance measures obtained with the chosen feature extraction and the classification procedures. The best performance measures obtained with respect to the chosen feature values are presented in Table 3. Table 3 shows that CuT+KNN, DTCWT+KNN, and ST + KNN offered better values of accuracy, precision, sensitivity, specificity, and F1 score as compared to alternative methods.

Our results suggest that the performance measures attained with the CoT, CWT and DWT are moderate as compared to CuT, DTCWT, and ST, and that the measures of EWT underperform. Figure 4 depicts the graphical representation of the performance measures computed with the clinical dataset. For this dataset, CuT+KNN, DTCWT+KNN and ST + KNN offer enhanced results.

Table 3 as well as Fig. 4 suggest that the CuT, DTCWT and ST approaches offer enhanced results on the clinical dataset as compared to the alternative methods considered in this research work. The performance of CuT+KNN, DTCWT+KNN, and ST + KNN are further examined using  $256 \times 256$  pixel sized T2-weighted brain MRI from the Harvard Brain Atlas [41]. Figure 5 depicts the sample test images considered for the study. Figure 5a presents the  $256 \times 256$  sized normal brain MRI and Fig. 5b depicts the brain image for the AD case (18 normal + 48 AD = 66 images). The assessment procedures, including CuT+KNN, DTCWT+KNN, and ST + KNN, are considered for the benchmark dataset, and corresponding results are depicted in Table 4 and Fig. 6. In this work, the training of the KNN classifier was performed with 55 images (15 normal and 40 AD cases) and validation is executed with 11 images (3 normal and 8 AD case) as discussed in Ayadi et al. [58].

From Table 4, it can be observed that the ST + KNN technique offers enhanced results with a lesser number of image features as compared to CuT+KNN and DTCWT+KNN, which require six and eight image features, respectively. From these results, it can be verified that the ST + KNN technique offers a better evaluation of the MRIs for normal versus the AD case. Furthermore, this approach requires minimal

**Table 5** Performance evaluation of the proposed and existing work on Harvard AD and normal database

Number of images	Author	Classifier	Accuracy (%)	Sensitivity (%)	Specificity (%)	Precision (%)
66	Ayadi et al. [58]	SVM (linear)	100	100	100	100
66		SVM (radial)	100	100	100	100
66		SVM (polynomial)	95.45	100	83.33	94.11
66		KNN	100	100	100	100
66		RF	83.33	81.25	66.66	86.66
66		Adaboost	83.33	89.58	89.58	87.75
66	This work	CuT+KNN	96.97	97.22	96.67	97.22
66		DTCWT+KNN	95.45	94.44	96.67	97.14
66		ST + KNN	98.48	96.97	100.00	100.00

image features to achieve better accuracy as compared to other techniques implemented in this research work.

Selection of dominant features for the selected method is depicted in Fig. 6, and the selected number of features is presented in Table 4. The CuT+KNN technique offered a better result when six features were considered for classification. The DTCWT+KNN and ST+KNN offered better results when five features were considered. Table 4 also shows that the ST+KNN technique provides better classification performance measures as compared to the alternatives.

The performance indices, including accuracy, precision, sensitivity, specificity, and F1 score, are considered to evaluate the adopted feature extraction techniques. The results presented in Fig. 7 suggest that the proposed techniques are efficient in attaining better performance values (>95.4%) on the considered dataset. This result also suggests that ST+KNN outperforms other feature extraction procedures by providing an enhanced performance index. The experimental outcome of this study verifies that the proposed CABD system offers satisfactory results in the quantitative analysis of the clinical as well as the benchmark datasets.

Comparison of proposed work with the existing work of Ayadi et al. [58] is depicted in Table 5. This table presents the classification accuracies obtained with various classifiers on the benchmark MRI dataset [41]. In Ayadi's work, a novel hybrid methodology with MRI pre-processing based on the median filter, DWT based image decomposition, feature extraction with GLCM/SIFT/SURF/Dense/FAST, implementation of the Bag-of-Words (BoW) concept and finally classification is proposed. However, it requires additional computation to implement the proposed technique. The author also provided a detailed comparative analysis using SVM, KNN, Random-Forest (RF) and Adaboost. The existing results were compared with our proposed methodology, and the comparative results are depicted in Table 5. The number of test images and dataset are the same in both cases. The results of Ayadi's hybrid approach are favourable in SVM (linear and radial) and the KNN case as compared to the proposed technique. The proposed ST+KNN approach offers better outcome as compared to the SVM (polynomial), RF and Adaboost. The proposed approach requires very few implementation steps in comparison to the hybrid approach described in the literature.

Furthermore, the proposed ST+KNN's classification accuracy was then compared with other related methods discussed by Chaplot et al. (2006) [59] and Zhang and Lenan (2012) [60], as depicted in Table 6.

The work of Chaplot et al. (2006) implements a feature extraction and classification of the Harvard Brain Atlas (<http://www.med.harvard.edu/aanlib/>) database

**Table 6** Existing works and their accuracy on the benchmark MRI dataset

Methods	Accuracy (%)
DWT + SOM [59]	94.00
DWT + SVM [59]	96.15
DWT + SVM + RBF [59]	98.00
DWT + PCA + SVM [60]	96.01
DWT + PCA + SVM + HPOL [60]	98.34
ST + KNN (This work)	98.48

using DWT, SVM, and Self-organizing maps (SOM). From the Table, it can be noted that the proposed approach (ST+KNN) offers a favourable result as compared to the existing method. Furthermore, the work of Zhang and Lenan (2012) considers a similar brain MRI database and presents a relative study among the classification accuracies of various SVM kernels. This work integrates DWT, PCA, and SVM techniques for feature extraction, selection and classification of the chosen brain MRI dataset. This Table also suggests that the accuracy obtained with our proposed method is favourable as compared with existing techniques, and better than the accuracy of hybrid feature extraction and classification procedure "DWT + PCA + SVM + HPOL" discussed by Zhang and Lenan [60].

In the proposed work, a machine learning technique is implemented to evaluate and classify the considered brain MRI slices into normal and AD classes. In recent years, deep learning techniques have been widely adopted by researchers to examine a class of medical images [61–64]. In the future, a suitable deep learning technique can be proposed to classify the considered brain MRI dataset, and its performance can be confirmed versus the ST+KNN approach discussed in the proposed work.

## Conclusion

Herein, an investigation of the axial images of T2-weighted brain MRI, with and without Alzheimer's disease (AD), were comparatively examined. The main objective of the study was to develop an efficient CABD system to assess the severity of brain abnormality caused by AD, without resorting to manual techniques that are slower to implement and that may be cost prohibitive when providing supportive care. A detailed evaluation of the existing feature extraction procedures is also presented, and feature selection is implemented using Student's t-test. The outcome of this work confirms that the ST+KNN technique offers an improved result as compared

to alternatives. Moreover, the number of features required for the ST + KNN is few (four) as compared with other techniques. The proposed paradigm offered better results on the brain MRI obtained from the medical clinic and the benchmark AD dataset. The performance of this system can be improved by replacing the KNN with other classifiers. In future work, instead of utilizing KNN, other classification techniques, such as SVM, neural-networks, random forest, and AdaBoost will be implemented, so that the CABD system's performance can be enhanced. Furthermore, a suitable deep learning model can be proposed to enhance classification accuracy.

### Compliance with ethical standards

**Conflict of interest** The authors declare that they have no conflict of interest.

**Ethical Approval** All procedures performed in studies involving human participants were in accord with the ethical standards of the institutional and/or national research committee (MREC ID No. 2017112–5771) and with the 1964 Helsinki declaration and its later amendments or comparable ethical standards.

### References

- World Health Organization (2018) The top 10 causes of death. <https://www.who.int/news-room/fact-sheets/detail/the-top-10-causes-of-death>
- Head, E., Powell, D., Gold, B. T., and Schmitt, F. A., Alzheimer's disease in down syndrome. *European Journal of Neurodegenerative Diseases* 1(3):353–364, 2012.
- Wang, T., Qiu, R. G., and Yu, M., Predictive modeling of the progression of Alzheimer's disease with recurrent neural networks. *Sci. Rep.* 8:9161, 2018. <https://doi.org/10.1038/s41598-018-27337-w>.
- Haaksma, M. L. et al., Comorbidity and progression of late onset Alzheimer's disease: A systematic review. *PLoS One* 12(5): e0177044. <https://doi.org/10.1371/journal.pone.0177044>.
- Malik, G. A., and Robertson, N. P., Treatments in Alzheimer's disease. *J. Neurol.* 264(2):416–418, 2017.
- Editorial, The three stages of Alzheimer's disease. *Lancet* 377(9776):1465, 2011. [https://doi.org/10.1016/S0140-6736\(11\)60582-5](https://doi.org/10.1016/S0140-6736(11)60582-5).
- Neugroschl, J., and Wang, S., Alzheimer's disease: Diagnosis and treatment across the spectrum of disease severity. *Mt Sinai J. Med.* 78(4):596–612, 2011. <https://doi.org/10.1002/msj.20279>.
- Pich, M. et al., Imaging as a biomarker in drug discovery for Alzheimer's disease: is MRI a suitable technology? *Alzheimers Res. Ther.* 6:51, 2014. <https://doi.org/10.1186/alzrt276>.
- Braskie, M. N., Toga, A. W., and Thompson, P. M., Recent advances in imaging alzheimer's disease. *J. Alzheimers Dis.* 33(1): S313–S327, 2013. <https://doi.org/10.3233/JAD-2012-129016>.
- Ossenkoppele, R. et al., Prevalence of Amyloid PET Positivity in Dementia Syndromes A Meta-analysis. *J. Am. Med. Assoc.* 313(19):1939–1949, 2015. <https://doi.org/10.1001/jama.2015.4669>.
- Norfray, J. F., and Provenzale, J. M., Alzheimer's disease: neuro-pathologic findings and recent advances in imaging. *Am. J. Roentgenol.* 182(1):3–13, 2004. <https://doi.org/10.2214/ajr.182.1.1820003>.
- Whalley, L. J., Spatial distribution and secular trends in the epidemiology of Alzheimer's disease. *Neuroimaging Clin. N. Am.* 22(1): 1–10, 2012. <https://doi.org/10.1016/j.nic.2011.11.002>.
- Stonington, C. M. et al., Predicting clinical scores from magnetic resonance scans in Alzheimer's disease. *NeuroImage* 5(4):1405–1413, 2010. <https://doi.org/10.1016/j.neuroimage.2010.03.051>.
- Liu, X. et al., Locally linear embedding (LLE) for MRI based Alzheimer's disease classification. *NeuroImage* 83:148–157, 2013. <https://doi.org/10.1016/j.neuroimage.2013.06.033>.
- Dimitriadis, S. I., Liparas, D., and Tsolaki, M. N., Random forest feature selection, fusion and ensemble strategy: Combining multiple morphological MRI measures to discriminate among healthy elderly, MCI, cMCI and Alzheimer's disease patients: From the alzheimer's disease neuroimaging initiative (ADNI) database. *J. Neurosci. Methods* 302:14–23, 2018. <https://doi.org/10.1016/j.jneumeth.2017.12.010>.
- Beheshti, I., Demirel, H., and Matsuda, H., Classification of Alzheimer's disease and prediction of mild cognitive impairment-to-Alzheimer's conversion from structural magnetic resonance imaging using feature ranking and a genetic algorithm. *Comput. Biol. Med.* 83:109–119, 2017. <https://doi.org/10.1016/j.combiomed.2017.02.011>.
- Westman, E., Muehlboeck, J.-S., and Simmons, A., Combining MRI and CSF measures for classification of Alzheimer's disease and prediction of mild cognitive impairment conversion. *NeuroImage* 62:229–238, 2012. <https://doi.org/10.1016/j.neuroimage.2012.04.056>.
- Sotensen, L., and Nielsen, M., Ensemble support vector machine classification of dementia using structural MRI and mini-mental state examination. *J. Neurosci. Methods* 302:66–74, 2018. <https://doi.org/10.1016/j.jneumeth.2018.01.003>.
- Casanova, R. et al., Using high-dimensional machine learning methods to estimate an anatomical risk factor for Alzheimer's disease across imaging databases. *NeuroImage* 183:401–411, 2018. <https://doi.org/10.1016/j.neuroimage.2018.08.040>.
- Calsolaro, V., and Edison, P., Neuroinflammation in Alzheimer's disease: Current evidence and future directions. *Alzheimer's and Dementia* 12(6):719–732, 2016.
- N. A. Mathew, R. Vivek, and P. Anurenjan, Early Diagnosis of Alzheimer's Disease from MRI Images Using PNN, in 2018 International CET Conference on Control, Communication, and Computing (IC4), pp. 161–164, 2018.
- Varatharajan, R., Manogaran, G., Priyan, M., and Sundarasekar, R., Wearable sensor devices for early detection of Alzheimer disease using dynamic time warping algorithm. *Clust. Comput.* 21(1):681–690, 2017.
- Dickerson, B., Stoub, T., Shah, R., Sperling, R., Killiany, R., Albert, M. et al., Alzheimer-signature MRI biomarker predicts AD dementia in cognitively normal adults. *Neurology* 76:1395–1402, 2011.
- C. Patil, M. Mathura, S. Madhumitha, S. S. David, M. Fernandes, A. Venugopal, et al., Using Image Processing on MRI Scans, in Signal Processing, Informatics, IEEE International Conference on Communication and Energy Systems (SPICES), pp. 1–5, 2015, 2015. <https://doi.org/10.1109/SPICES.2015.7091517>.
- Kaur, A., and Kaur, P., A comparative study of various exudate segmentation techniques for diagnosis of diabetic retinopathy. *International Journal of Current Engineering and Technology* 46: 142–146, 2016.
- Zhao, Y., Raichle, M. E., Wen, J., Benzinger, T. L., Fagan, A. M., Hassenstab, J. et al., In vivo detection of microstructural correlates of brain pathology in preclinical and early Alzheimer Disease with magnetic resonance imaging. *Neuroimage* 148:296–304, 2017.

27. Sankari, Z., and Adeli, H., Probabilistic neural networks for diagnosis of Alzheimer's disease using conventional and wavelet coherence. *J. Neurosci. Methods* 197(1):165–170, 2011. <https://doi.org/10.1016/j.jneumeth.2011.01.027>.
28. Plant, C., Teipel, S. J., Oswald, A., Böhm, C., Meindl, T., Mourao-Miranda, J. et al., Automated detection of brain atrophy patterns based on MRI for the prediction of Alzheimer's disease. *Neuroimage* 50:162–174, 2010.
29. Zhang, Y., Wang, S., Sui, Y., Yang, M., Liu, B., Cheng, H. et al., Multivariate approach for Alzheimer's disease detection using stationary wavelet entropy and predator-prey particle swarm optimization. *J. Alzheimers Dis.* 65:855–869, 2018.
30. Wang, S.-H., Zhang, Y., Li, Y.-J., Jia, W.-J., Liu, F.-Y., Yang, M.-M. et al., Single slice based detection for Alzheimer's disease via wavelet entropy and multilayer perceptron trained by biogeography-based optimization. *Multimed. Tools Appl.* 77(9):10393–10417, 2016.
31. Zhang, Y., Wang, S., and Dong, Z., Classification of Alzheimer disease based on structural magnetic resonance imaging by kernel support vector machine decision tree. *Prog. Electromagn. Res.* 144: 171–184, 2014.
32. Zhang, Y., and Wang, S., Detection of Alzheimer's disease by displacement field and machine learning. *Peer J* 3:e1251, 2015.
33. El-Dahshan, E.-S. A., Hosny, T., and Salem, A.-B. M., Hybrid intelligent techniques for MRI brain images classification. *Digital Signal Processing* 20:433–441, 2010.
34. Wang, S.-H., Du, S., Zhang, Y., Phillips, P., Wu, L.-N., Chen, X.-Q. et al., Alzheimer's disease detection by pseudo Zernike moment and linear regression classification. *CNS & Neurological Disorders-Drug Targets (Formerly Current Drug Targets-CNS & Neurological Disorders)* 16:11–15, 2017.
35. Gorji, H. T., and Haddadnia, J., A novel method for early diagnosis of Alzheimer's disease based on pseudo Zernike moment from structural MRI. *Neuroscience* 305:361–371, 2015.
36. Wang, S., Zhang, Y., Liu, G., Phillips, P., and Yuan, T.-F., Detection of Alzheimer's disease by three-dimensional displacement field estimation in structural magnetic resonance imaging. *J. Alzheimers Dis.* 50:233–248, 2016.
37. Zhang, Y., Dong, Z., Phillips, P., Wang, S., Ji, G., Yang, J. et al., Detection of subjects and brain regions related to Alzheimer's disease using 3D MRI scans based on eigenbrain and machine learning. *Front. Comput. Neurosci.* 9:66, 2015.
38. Zhang, Y., Wang, S., Sun, P., and Phillips, P., Pathological brain detection based on wavelet entropy and Hu moment invariants. *Biomed. Mater. Eng.* 26:S1283–S1290, 2015.
39. Hett, K., Ta, V.-T., Manjón, J. V., and Coupé, P., Adaptive fusion of texture-based grading for Alzheimer's disease classification. *Comput. Med. Imaging Graph.* 70:8–16, 2018. <https://doi.org/10.1016/j.compmedimag.2018.08.002>.
40. Gao, X. W., Hui, R., and Tian, Z., Classification of CT brain images based on deep learning networks. *Comput. Methods Prog. Biomed.* 138:49–56, 2017.
41. Johnson, K.A., and Becker J.A. The whole brain atlas. Available from Harvard Medical School, USA <http://www.med.harvard.edu/aanlib/>
42. Zhu, Y., and Huang, C., An improved median filtering algorithm for image noise reduction. *Phys. Procedia* 25:609–616, 2012.
43. Acharya, U. R., Sree, S. V., Ang, P. C. A., Yanti, R., and Suri, J. S., Application of non-linear and wavelet based features for the automated identification of epileptic EEG signals. *Int. J. Neural Syst.* 22(02):1250002, 2012. <https://doi.org/10.1142/S0129065712500025>.
44. Zhou, N., and Wang, L., A Modified T-test Feature Selection Method and Its Application on the Hap Map Genotype Data. *Genomics Proteomics Bioinformatics* 5(3–4):242–249, 2007. [https://doi.org/10.1016/S1672-0229\(08\)60011-X](https://doi.org/10.1016/S1672-0229(08)60011-X).
45. Chandra, B., and Gupta, M., An efficient statistical feature selection approach for classification of gene expression data. *J. Biomed. Inform.* 44(4):529–535, 2011. <https://doi.org/10.1016/j.jbi.2011.01.001>.
46. Rajinikanth, V., Satapathy, S. C., Fernandes, S. L., and Nachiappan, S., Entropy based segmentation of tumor from brain MR images—a study with teaching learning based optimization. *Pattern Recogn. Lett.* 94:87–95, 2017. <https://doi.org/10.1016/j.patrec.2017.05.028>.
47. Raja, N. S. M., Fernandes, S. L., Dey, N., Satapathy, S. C., and Rajinikanth, V., Contrast enhanced medical MRI evaluation using Tsallis entropy and region growing segmentation. *J. Ambient. Intell. Humaniz. Comput.:*1–12, 2018. <https://doi.org/10.1007/s12652-018-0854-8>.
48. Acharya, U. R., Sudarshan, V. K., Adeli, H., Santhosh, J., and Koh, J. E. W., A novel depression diagnosis index using nonlinear features in EEG signals. *Eur. Neurol.* 74(1–2):79–83.
49. Acharya, U. R., Faust, O., Sree, S. V., Molinari, F., Garberoglio, R., and Suri, J. S., Cost-Effective and Non-Invasive Automated Benign & Malignant Thyroid Lesion Classification in 3D Contrast-Enhanced Ultrasound Using Combination of Wavelets and Textures: A Class of ThyroScan™ Algorithms. *Technology in Cancer Research & treatment* 10(4):371–380, 2011.
50. Gudigar, A., Raghavendra, U., San, T. R., Ciaccio, E. J., and Acharya, U. R., Application of multiresolution analysis for automated detection of brain abnormality using MR images: A comparative study. *Futur. Gener. Comput. Syst.* 90:359–367, 2019.
51. Acharya, U. R., Fujita, H., Lih, O. S., Adam, M., Tan, J. H., and Chua, C. K., Automated detection of coronary artery disease using different durations of ECG segments with convolutional neural network. *Knowl.-Based Syst.* 132:62–71, 2017.
52. Jha, D., and Kwon, G.-R., Contourlet-based feature extraction for computer-aided classification of Alzheimer's disease. *Alzheimers and Dementia* 14(7):1473, 2018. <https://doi.org/10.1016/j.jalz.2018.06.2498>.
53. Krishnan, K. G., Vanathi, P. T., and Abinaya, R., Texture classification using Shearlet transform energy features. *Communications in Computer and Information Science* 679:3–13, 2016.
54. Lim, W.-Q., The discrete Shearlet transform: a new directional transform and compactly supported Shearlet frames. *IEEE Trans. Image Process.* 19(5):1166–1180, 2010. <https://doi.org/10.1109/TIP.2010.2041410>.
55. Lim, W.-Q., Nonseparable Shearlet transform. *IEEE Trans. Image Process.* 22(5):2056–2065, 2013. <https://doi.org/10.1109/TIP.2013.2244223>.
56. Selesnick, I. W., Baraniuk, R. G., and Kingsbury, N. C., The dual-tree complex wavelet transform. *IEEE Signal Process. Mag.* 22(6):123–151, 2005. <https://doi.org/10.1109/MSP.2005.1550194>.
57. Wang, S. et al., Dual-Tree Complex Wavelet Transform and Twin Support Vector Machine for Pathological Brain Detection. *Appl. Sci.* 6(6):169, 2016. <https://doi.org/10.3390/app6060169>.
58. Ayadi, W., Elhamzi, W., Charfi, I., and Atri, M., A hybrid feature extraction approach for brain MRI classification based on Bag-of-words. *Biomedical Signal Processing and Control* 48:144–152, 2019. <https://doi.org/10.1016/j.bspc.2018.10.010>.
59. Chaplot, S., Patnaik, L. M., and Jagannathan, N. R., Classification of magnetic resonance brain images using wavelets as input to support vector machine and neural network. *Biomedical Signal Processing and Control* 1(1):86–92, 2006.
60. Zhang, Y., and Lenan, W., An MR brain images classifier via principal component analysis and kernel support vector machine. *Prog. Electromagn. Res.* 130:369–388, 2012.

61. Tan, J. H., Acharya, U. R., Bhandary, S. V., Chua, K. C., and Sivaprasad, S., Segmentation of optic disc, fovea and retinal vasculature using a single convolutional neural network. *J. Comput. Sci.* 20:70–79, 2017.
62. Tan, J. H. et al., Automated segmentation of exudates, haemorrhages, microaneurysms using single convolutional neural network. *Inf. Sci.* 420:66–76, 2017.
63. Raghavendra, U. et al., Deep convolution neural network for accurate diagnosis of glaucoma using digital fundus images. *Inf. Sci.* 441:41–49, 2018.
64. Raghavendra, U., Bhat, N. S., Gudigar, A., and Acharya, U. R., Automated system for the detection of thoracolumbar fractures using a CNN architecture. *Futur. Gener. Comput. Syst.* 85:184–189, 2018.

**Publisher's Note** Springer Nature remains neutral with regard to jurisdictional claims in published maps and institutional affiliations.